PNAS Nexus, 2025, 4, pgaf200
https://doi.org/10.1093/pnasnexus/pgaf200
Advance access publication 14 June 2025
Research Report

Morula complementation restores male germline in *NANOS2* null sheep

Zachariah L. McLean[a,b,1], Lisanne M. Fermin[a,1], Sarah J. Appleby[a], Jingwei Wei[a], Fanli Meng[a], Paul H. Maclean[d], Benjamin J. Perry[c], Brigid Brophy[a], Pavla Turner[a], Blaise Forrester-Gauntlett[a], David N. Wells[a], Russell G. Snell[b] and Björn Oback[a,e,*]

[a]Animal Biotech, AgResearch Ltd, Ruakura Research Centre, Hamilton 3214, New Zealand
[b]Applied Translational Research Group and Centre for Brain Research, School of Biological Sciences, University of Auckland, Auckland 1010, New Zealand
[c]Bioinformatics, Analytics and Modelling, AgResearch, Invermay Agricultural Centre, Mosgiel 9053, New Zealand
[d]Statistics, AgResearch, Grasslands Research Centre, Palmerston North 4410, New Zealand
[e]Department of Molecular Medicine and Pathology, School of Medical Sciences, University of Auckland, Auckland 1142, New Zealand
*To whom correspondence should be addressed: Email: bjorn.oback@plantandfood.co.nz
[1]Z.L.M. and L.M.F. contributed equally to this work.
Edited By Christof Niehrs

Abstract

Current livestock breeding is slow to respond to rapidly mounting environmental pressures that threaten sustainable animal protein production. New approaches can accelerate genetic improvement by multiplying valuable embryonic, rather than adult genotypes. Chimeras, derived from complementing a sterile host with a fertile donor embryo, provide a pathway to multiply and exclusively transmit elite male germlines. We established genetically sterile hosts and optimized embryo complementation conditions to achieve absolute germline transmission in sheep. The spermatogonia-specific gene *NANOS2* was disrupted in male (*NANOS2*$^{+/-}$, *NANOS2*$^{-/-}$) and female (*NANOS2*$^{-/-}$) ovine fetal fibroblasts via gRNA–Cas9-mediated homology-directed repair. Targeted cell strains and wild-type controls were used to produce cloned offspring for breeding and phenotyping. Male homozygous knockout clones lacked detectable germ cells, while the somatic compartment of the testis remained intact. By contrast, male monoallelic and female biallelic targeting of *NANOS2* did not affect germline development, resulting in fertile animals capable of producing fertile offspring with normal reproductive performance. The germ cell niche in *NANOS2*$^{-/-}$ hosts was most efficiently complemented by aggregating compacted morulae, rather than earlier cleavage stages, resulting in 97% blastocyst chimerization. Embryo-complemented cloned lambs from two different donor cell lines showed variable chimerism across tissues from each germ layer, including various degrees of germline colonization. A subset of germline chimeras contained normal numbers of prospermatogonia, indicating that the germline was fully restored for absolute transmission of the donor cell genotype.

Keywords: *NANOS2*, livestock, spermatogonia, germline chimera, embryo complementation

Significance Statement

The male germline dominates genetic improvement in farm animal breeding. However, traditional breeding is slow to respond to rapidly changing environmental pressures that threaten animal protein production. To accelerate genetic improvement, we generated absolute elite germline transmitters in sheep. First, homozygous disruption of the *NANOS2* gene produced rams with normal testis but lacking sperm. Second, morula complementation filled the vacant germline niche in chimeric lambs and restored normal numbers of male germ cells. Importantly, heterozygous males and homozygous females were fertile, providing a pathway for continuous supply of genetically sterilized host embryos by breeding. These findings advance a breeding approach that integrates embryo-based complementation with genomic selection for exclusive dissemination of selected embryo genotypes.

Introduction

Animal breeding achieves genetic progress mainly by controlling the male germline through various assisted reproductive technologies, including artificial insemination (AI). Compared with natural mating, AI multiplies the number of offspring from high genetic merit sires by three to four orders of magnitude, accounting for ~50% of the increase in productivity per animal in US dairy cattle (1). Insemination-based breeding strategies have been genetically improving livestock by 1–3% p.a. for decades. However, this incremental progress is slow to respond to rapidly mounting

Competing Interest: L.M.F., J.W., F.M., P.T., B.B., P.H.M., B.J.P., B.F.-G., D.N.W., and B.O. are employees of AgResearch Ltd. The authors declare no competing interests.
Received: January 20, 2025. **Accepted:** May 29, 2025

environmental pressures that threaten food security from sustainable animal protein production. Furthermore, AI is invasive, labor-intensive, and costly in sheep breeding, which mainly relies on natural mating instead (2). This obstructs rapid gains in efficiency and sustainability of sheep production compared with dairy cattle breeding.

New approaches promise to accelerate breeding by producing male chimeras, composite animals comprising a sterile host, and fertile donor component, with the latter exclusively engendering the male germline. Such chimeric sires with fully defined elite donor germlines, referred to as "absolute transmitters," could produce high genetic value sperm for natural mating and reduce the genetic lag between the elite seedstock sector and the commercial sector (3).

Two approaches currently compete for producing animal chimeras (4). Both rely on complementing an infertile genotype with a fertile donor, by adding either germline-competent embryonic cells to early embryos or spermatogonial stem cells to the testis. In both cases, the germline is first deleted and then restored with the desirable donor genetics. Several mutations specifically eliminate germ cells while maintaining an intact testicular niche, providing suitable germline-ablated hosts for complementation. These include transcriptional regulators *Etv5* (5), *Prdm14* (6), and *Tsc22d3* (7–9), as well as RNA-binding proteins *DAZL* and *NANOS* (10–15). Without *Nanos2*, male germ cells in mice are removed by apoptosis (16), with no germ cells detectable upon puberty (17). Crucially, *NANOS2* mutations only affect fertility in homozygous male mutants, while females and heterozygous males are fertile (10, 12). Unlike other targets, this would allow breeding homozygous mutant females with heterozygous mutant males to efficiently produce sterile homozygous male hosts for germline complementation and absolute transmission of male donor genetics.

Some mutants were successfully used as sterile hosts for germline complementation. Testis complementation was performed on *Tsc22d3* (9), *Dazl* (13), and *Nanos2* (10) knockout hosts with the resulting "surrogate sires" producing only sperm from the donor male. Embryo complementation with either blastomeres or embryonic stem cell (ESC) donors has been extensively used in mice to colonize the germline after reintroducing them into an embryonic host, by either aggregation or injection. Production of aggregation chimeras in livestock has followed the murine model, despite species-specific differences in the timing of early developmental events. Sheep and cattle embryos were either aggregated as 4–8 cells (18, 19) or 32–64 cells, equivalent to the morula stage (20), but the optimal aggregation timing in ruminants remains to be determined.

Blastomere-derived germline chimeras were produced in pigs (21), while livestock ESCs have so far only engendered somatic cell lineages in pigs (22) and cattle (23). Embryo complementation into germline-ablated hosts was reported for *Tsc22d3* (7, 8), *Nanos3* (11, 15), and *Prdm14* (6) knockouts.

Here, we used gRNA–Cas9 to mediate a homology-directed repair (HDR) biallelic loss-of-function mutation in *NANOS2*, ablating the male germline in cloned sheep but leaving the testicular soma intact. We observed no reproductive phenotype in homozygous knockout ewes and heterozygous rams, which were bred to provide a continuous supply of homozygous null host embryos. The morula stage was optimal for producing chimeric blastocysts and restoring the germline in absolute transmitter lambs. This opens the prospect of a novel breeding platform that integrates embryo-based complementation with genomic selection, multiplication, and gene modification to benefit agribiotechnology and species conservation.

Results

Germline ablation

Editing NANOS2 in ovine fetal fibroblasts

To disrupt the male germline, we targeted *NANOS2* (gene ID: 101115150, Fig. 1A). Three gRNAs with minimal predicted off-target sites were selected to introduce either a 5-bp insertion, resulting in a premature termination codon 18 nucleotides after the start of the coding sequence and a new diagnostic *TaqI* restriction site, or an 8-bp deletion, resulting in a frameshift mutation and production of a nonsense protein (Fig. 1B). Successful genome editing was confirmed by ddPCR with hydrolysis probes specific to the mutant allele and unrelated beta-casein (*CSN2*) reference gene. Biallelic HDR frequencies were 9.6% for gRNA1, 10.4% for gRNA2, and 7.1% for gRNA3 (Fig. S1a). Cell strains were isolated by manual selection of mitotic cells from the gRNA2-edited population. We screened 45 cell clones and obtained five PCR- and four sequence-validated *NANOS2*$^{-/-}$ cell strains (Table S1). Female HDR clones were isolated in a similar fashion, resulting in five sequence-validated clones. For isolating male heterozygous cell strains, 52 clones were screened for presence of one wild-type allele by ddPCR. From those, we identified 21 cell strains with one wild-type copy and validated three heterozygous nonhomologous end joining (NHEJ) clones, two of which grew well enough to be cryopreserved. Based on their growth and validated mutation profile, we selected four male HDR cell strains, one female HDR strain, and one male NHEJ strain for somatic cell transfer (SCT) cloning (Fig. S1b). We also screened for unintentional integration of the genome editors with a PCR-based screen for the Cas9 coding region, which revealed that two of the biallelically edited clonal male and one of the female cell strains, but none of the heterozygous male cell strains, had integrated the gRNA–Cas9 plasmid into their genome (Fig. S1c). To test specificity of the gRNA–Cas9 system, a biased Sanger sequencing screen of the top three potential off-target sites, as identified by CCTop, revealed no mutations in the homozygous male mutant (Fig. S1d).

Reproductive cloning of different NANOS2 genotypes

Homozygous male and female knockout cell strains, as well as heterozygous male and wild-type female donor cell strains, were chosen for somatic cell cloning, which is the fastest reproductive technology to generate fully defined founder genotypes (Table 1). Across numerous independent cloning runs, *NANOS2* edited and wild-type cell strains developed to the blastocyst stage at similar frequencies of 5–11%. Cloned blastocysts were freshly transferred into estrus synchronized ewes on day 7 of in vitro culture. In total, 6/54 (11%) male knockout lambs were produced with no significant differences between the different clonal cell strains. Of these lambs, two out of six survived past puberty into adulthood. Similar survival was observed in the heterozygous and homozygous female knockout groups with six and seven lambs born and one and three lambs, respectively, developing into adulthood. Development in the nonedited female control group was not significantly different with 11 lambs being born and four developing into adulthood.

For a more comprehensive off-target analysis, we sequenced the whole genome of one *NANOS2*$^{+/-}$ male lamb and its nonedited parental male fetal fibroblast (MFF) donors, as well as three *NANOS2*$^{-/-}$ female lambs and their corresponding wild-type female fetal fibroblast (FFF) donors (Fig. S2a). The average genome coverage was 32- to 80-fold, sufficient to detect both the heterozygous 8-bp deletion and homozygous 5-bp insertion in the cloned lambs (Table S2). Filtering criteria were applied to raw variant calls to identify potential off-target mutations and spontaneous

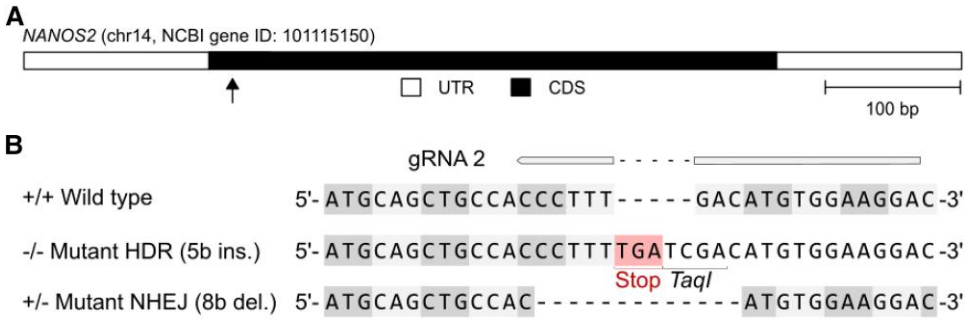

Fig. 1. Disrupting ovine *NANOS2*. A) Ovine *NANOS2* gene showing the 5′ untranslated region (UTR, white), single-exon coding sequence (CDS, black), and the Cas9/gRNA target site (arrow). Scale bar = 100 bp. B) gRNA2 directs Cas9 cleavage to create a frameshift in the *NANOS2* gene, either by either HDR-mediated 5 bp homozygous ($^{-/-}$) insertion of a stop codon (red) and *TaqI* restriction site or nonhomologous end joining (NHEJ)-mediated 8 bp (heterozygous $^{+/-}$) deletion. Alternating codons are indicated with dark and light gray shading, respectively, to highlight the indel mutations.

de novo mutations in the gene-edited donor cells and their cloned lamb descendants (Fig. S2b). Variants relative to the reference genome that were identified to be monomorphic were removed, which reduced the 16,904,969 and 16,354,796 variant sites to 912,546 and 1,304,166 for MFF and FFF, respectively. To address the probability of heterozygosity, we filtered for allele depth, decreasing numbers to 480,788 and 303,862, respectively. To remove polymorphic variants that are common to the wider sheep population, all variants that were segregating in the European Variant Archive v6 for *Ovis aries* were also removed, further reducing the number of variants to 410,337 and 269,961, respectively. Only the intersection of the resultant variants called from all three algorithms was taken for further analysis (53,462 and 31,232, respectively). Potential genome-wide off-target sites were predicted based on on-target sequence similarity using fuzznuc and CRISPOR, where we allowed for up to five mismatches with the on-target site. This identified 10 and 12 overlapping variants, respectively, from 943 potential off-targets within ±100 bp of the target sites. Variants with a map quality score of <60, as well as the actual on-target gene edits, were removed. The remaining 12 candidate off-target mutations were manually examined by visualization of sequence reads in the Integrative Genomics Viewer (IGV). We did not detect any shared off-target mutations in the genome of HDR-edited lambs (#1927, #1936, and #1938). One NHEJ-edited lamb (#1945) showed three single-nucleotide changes, which were not present in the parental donor cells, and could be either an off-target or a de novo mutation.

Potential de novo mutations happen after the editing and are unique to each cloned animal, resulting in 1,773, two, one, and three variants for #1945, #1927, #1936, and #1938, respectively. After filtering for map quality, allele depth, and excluding the correct on-target edits, this number reduced to 436 and 0 for MFF and FFF-derived clones, respectively. These putative de novo mutations showed no overlap with the predicted off-target sites and have likely arisen after the editing events, during either cell culture or cloned lamb development.

Phenotype of different NANOS2 sheep clones

To evaluate gene expression differences, testes were harvested from deceased neonate *NANOS2*$^{-/-}$ ($n = 3$ lambs), *NANOS2*$^{+/-}$ ($n = 4$), and cloned wild-type controls ($n = 3$). Mutant testis parenchyma abolished or strongly reduced germ cell-specific expression (*DAZL*, *SALL4*, *DDX4*, *NANOS2*, *LIN28*, and *NANOG*) compared with wild type (Fig. 2A). By contrast, somatic gene expression did not differ between the three genotypes, including markers for Sertoli cells (*SOX9*, *WT1*, and *FSHR*); Sertoli and peritubular myoid cells (*GDNF*); Sertoli and Leydig cells (*GATA4* and *NR5a1*); Leydig cells (*INSL3*, *HSD3B1*, and *STAR*); Leydig and peritubular myoid (*CSF1*); peritubular myoid cells (*ACTA2*); and peritubular myoid cells and blood vessels (*MYH11*). All germ cell markers were significantly down-regulated in homozygous compared with heterozygous animals, while there were no differences in the somatic compartment, except for GATA4, which appeared slightly down-regulated in the homozygous mutant (Fig. 2B).

To validate the gene expression results with histological and protein data, testes harvested from the deceased lambs were histologically analyzed. Compared with *NANOS2*$^{+/+}$ and *NANOS2*$^{+/-}$, *NANOS2*$^{-/-}$ lambs comprised somatic support cells in the testis but lacked prospermatogonia and sperm (Fig. 2C). Immunostaining on cryosections showed no signal for germ cell markers DDX4 and SSEA4 in the center of the testis cords for *NANOS2*$^{-/-}$ lambs, with clear presence of both antigens in wild-type and heterozygous animals. In contrast to the prospermatogonial markers, Sertoli cell marker SOX9, Sertoli/Leydig marker GATA4, and Leydig cell marker 3β-HSD were all present in *NANOS2*$^{-/-}$, *NANOS2*$^{+/-}$, and *NANOS2*$^{-/-}$ lambs. Actin filament staining also showed the same pattern for all genotypes with strong signals from the peritubular myoid cells and blood vessel walls around the testis cords. Most discriminatory, there were no spermatozoa detectable in fresh ejaculates of an adult knockout ram. Sperm quality in a heterozygous ram, on the contrary, was not affected in terms of viability, motility, and postthaw survival (Table 2). Sperm collected from a *NANOS2*$^{+/-}$ ram were fully competent to fertilize oocytes after in vitro fertilization (IVF) and AI/natural mating, resulting in similar numbers of in vitro produced embryos and lambs, respectively, as wild-type sperm. We conclude that the introduced biallelic *NANOS2* loss-of-function mutation led to a germ cell-deficient male phenotype without compromising development of somatic support cells, while the monoallelic *NANOS2* mutation did not affect germline development.

In females, biallelic *NANOS2* deletion did not affect the histology of ovaries at different stages of peri- and postnatal development compared with wild type (Fig. S3a). Quantification of follicle numbers at different stages of maturity (primordial, primary, secondary, Graafian) did not reveal any significant changes between knockout and wild type (Fig. S3b). Oocyte recovery after ovum pick-up (OPU) was normal in four different *NANOS2*$^{-/-}$ female clones, yielding similar numbers of follicles and oocytes per OPU donor as isogenic wild-type control clones (Table 3). The knockout oocytes were fully competent and resulted in similar numbers of embryos after IVF with *NANOS2*$^{+/-}$ sperm as wild-type oocytes (Table 4).

Table 1. Cloning efficiency of *NANOS2* genotypes.

NANOS2	Cell line	Breed	Sex	nIVC[a]	B (%)[b–e]	nET[f]	No. of lambs (%)[g]	No. of adults (%)[g]
−/−	MFF[b]	Composite	Male	1,704	118 (7)	54	6 (11)	2 (4)
+/−	MFF[c]	Composite	Male	763	87 (11)	45	6 (13)	1 (2)
−/−	FFF[d]	Poll Dorset	Female	1,467	88 (6)	55	7 (13)	3 (6)
+/+	FFF	Poll Dorset	Female	1,432	71 (5)	43	11 (26)	4 (9)

[a]Number of embryos placed into in vitro culture (nIVC).
[b]Clonal MFF strains 12, 19, 31, and 33.
[c]Clonal MFF strains 72 and 127.
[d]Clonal FFF strains 6 and 22.
[e]nIVC that developed into morphological grade 1–3 blastocysts ($B^{a–c}$).
[f]Number of $B^{a–c}$ transferred (nET).
[g]Normalized on nET.

Producing viable NANOS2 "host breeders"

We started breeding the cloned founder animals to propagate their genotypes. Oocytes were recovered from *NANOS2*$^{-/-}$ (*ins5 bp/ins5 bp*) and wild-type cloned females and in vitro fertilized them with *NANOS2*$^{+/-}$ (*+/Δ8 bp*) sperm (Table 5). The resulting 36 embryos (25 from $^{+/+}\times^{+/-}$ and 11 from $^{-/-}\times^{+/-}$ matings) were transferred into 12 gestational surrogates. At term, 11 lambs (six males and five females) were born (seven alive and four dead). There was no difference between survival of the embryos derived from knockout vs. wild-type oocytes, demonstrating that biallelic *NANOS2* knockout does not compromise reproductive performance in vivo. All lambs were genotyped by ddPCR with wild-type and different mutant *NANOS2* probes (Table S3). We obtained one *NANOS2*$^{-/-}$, five *NANOS2*$^{+/-}$, and five wild-type lambs, close to the expected numbers after Mendelian segregation (predicted 1.7 *NANOS2*$^{-/-}$, 5.5 *NANOS2*$^{+/-}$, and 3.8 wild-type lambs). This enables stable maintenance of the necessary *NANOS2* genotypes to provide a continuous supply of homozygous host breeders and in vitro production (IVP)-derived host embryos in the future.

Germline complementation

IVP of chimeric blastocysts

To produce fluorescent reporter donors for lineage tracing in chimeras, MFFs were transfected with the CAGGS-mCherry/PGK-PuroR plasmid and the hyperactive *Sleeping Beauty* transposase. *CAGGS-mCherry* cell strains (#5 and #9) were selected on mCherry brightness (Fig. S4a). Flow cytometry showed that both cell strains were clonal, while another candidate strain (#7) was of mixed origin (Fig. S4b). *mCherry* expression tended to be higher in cell strain #9 (Fig. S4c), which was consistent with this strain carrying eight transgene copies, compared with three copies in strain #5 (Fig. S4d). Candidate *CAGGS-mCherry* cell strains were used as nuclear donors for SCT cloning. All live blastocysts derived from *CAGGS-mCherry* donor cells were uniformly red fluorescent above background (Fig. S4e). Chimeric embryos were produced by disaggregating *NANOS2*$^{-/-}$ SCT reconstructed embryos and reaggregating them with a disaggregated *CAGGS-mCherry* embryo. Aggregations were carried out on days 3 (D3), 4 (D4), and 5 (D5) of in vitro culture (Fig. S4f). The embryos used for aggregation had 11.4 ± 3.3 (D3) or 18.1 ± 6.0 (D4) blastomeres or were compacting (D5), representing the 8–16-cell stage, 16–32-cell stage, and compacted morula stage, respectively. Following initial characterization of the donor cells and aggregation procedure, chimerism in D7 blastocysts was scored by red fluorescent signal strength (Fig. 3A), indicating putative chimerism, and size (1× or 2×). Using this subjective categorizing, the proportion of blastocysts with medium mCherry signal, i.e. putative chimeras, was increased in the 2× vs. 1× group across each aggregation stage (Fig. 3B). Irrespective of size, the proportion of putative chimeric blastocysts was highest when aggregation occurred at the morula stage. Subjective categorization of chimerism was validated on a subset of blastocysts from aggregated embryos using ddPCR with hydrolysis probes to identify the wild type. Again, the proportion of putative chimeras was increased in the 2× vs. 1× group across each aggregation stage, confirming size as a good proxy for chimerism (Fig. 3C). Overall, in vitro chimerization was highest with embryos aggregated at the morula stage, resulting in 97% (37/38) of aggregated embryos categorized as chimeras, compared with 13% (4/30) at D4 and 5% (4/136) on D3 (Table 5). Incomplete incorporation of blastomeres sometimes resulted in two blastocysts arising from one aggregate with different frequencies on D3, D4, and D5 (6/136 = 4%, 0/30 = 0%, and 6/38 = 16%, respectively). This accounts for the >100% blastocyst development after morula aggregation (Table 6).

Generating clone↔clone chimeric lambs for absolute germline transmission

Aggregated blastocysts were transferred into estrus synchronized ewes on day 6 or 7 of in vitro culture. As donors, we used either *mCherry* reporter cells or nontransgenic adult ear skin fibroblasts from an elite Texel ram. SCT embryos from either donor line were aggregated with stage-matched *NANOS2*$^{-/-}$ SCT embryos. Both donor cell types produced cloned lambs but only those from the Texel donor survived into adulthood. Chimerism was determined using ddPCR of tissues representing each germ layer (brain, kidney, liver, and testis) and histological assessment of germ cells in deceased neonates and live animals. Both methods identified one chimeric lamb among the mCherry-derived donors and several chimeras from the elite Texel donor line (Table 7). Using subjective categorization of mCherry fluorescence, we predicted that none of the lambs from 8–16-cell stage aggregates and all the lambs from compacted morula aggregates would be chimeric. One fetus from the 8–16-cell stage aggregates developed hydroallantois and was recovered at D114 of gestation (aggregate #1). A recipient carrying twins from 8–16-cell stage aggregates gave birth on D148, but one lamb was dead (aggregate #2) and the other died within 30 min (aggregate #3). The fetus from the compacted morula aggregate aborted on day 133 of gestation (aggregate #4). As predicted, PCR analysis for the *NANOS2* wild-type allele confirmed that only aggregate lamb #4 was chimeric (Fig. 4A). Testes harvested from the four lambs were histologically analyzed. Testis from putative nonchimeric aggregate lamb 1 infrequently contained spermatogonia, while lambs 3 and 4 lacked spermatogonia. The density of prospermatogonia in testis sections of this chimeric lamb was similar to an age-matched cloned wild-type control (491.3 ± 157.4 vs. 489.5 ± 149.1,

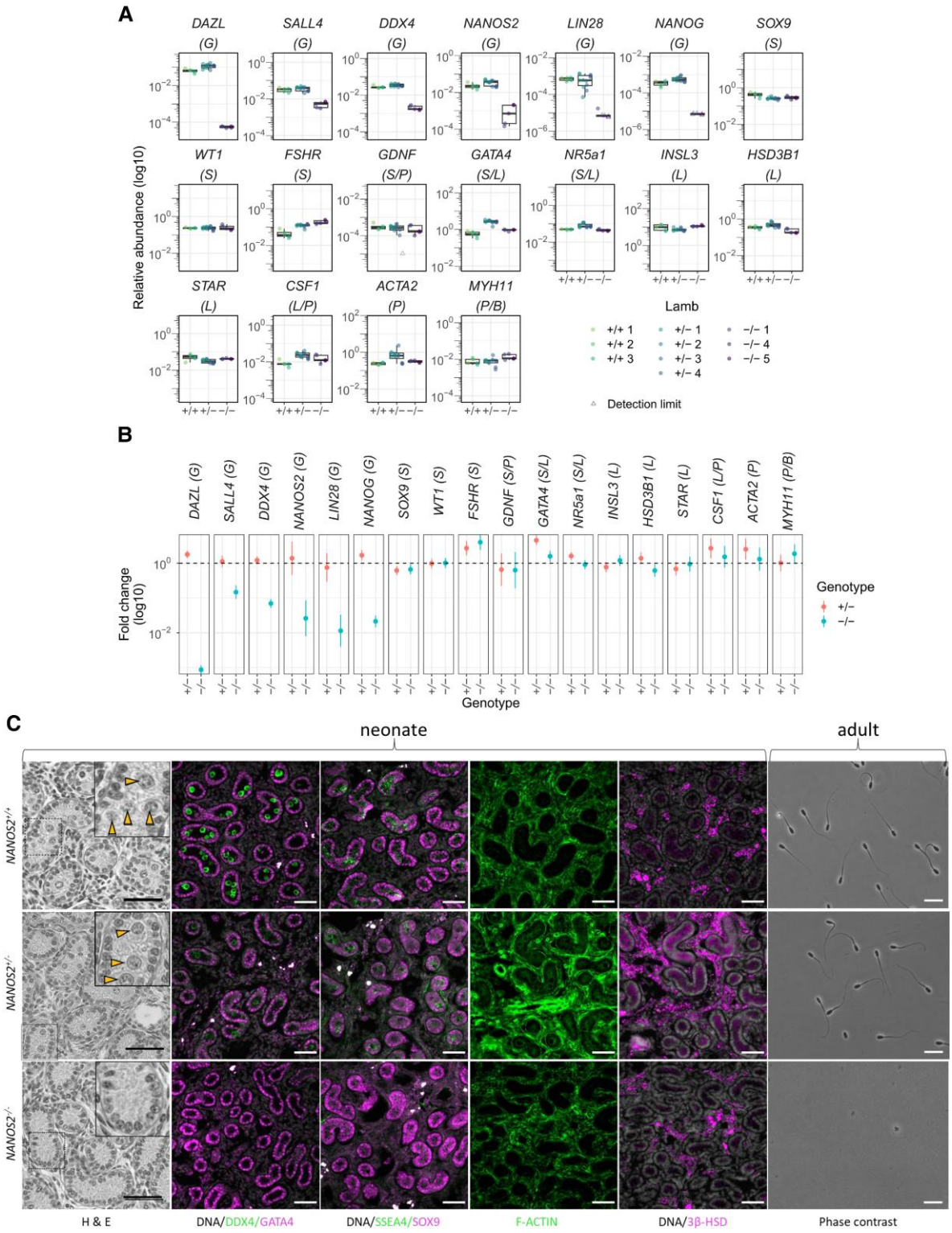

Fig. 2. Gene expression changes in *NANOS2* mutant testes. Lambs have reduced germ cell signature but unaltered somatic markers. A) Gene expression in testis parenchyma of wild-type ($^{+/+}$), heterozygous ($^{+/-}$), and homozygous ($^{-/-}$) mutant lambs ($\log_{10}$ axis). The relative expression of various genes is shown for different lineages indicated by an abbreviation in brackets. They represent prospermatogonial germ cells (G), Sertoli cells (S), peritubular myoid cells (P), Leydig cells (L), and blood vessels (B). The vertical point range indicates the 95% CI for the estimated marginal mean. Filled circles indicate detected transcript, while open triangles represent a negative result (no amplification or wrong melting peak), indicating the detection limit. A C_q value of 35 was given for missing values for computation of the baseline relative expression. Different color shades represent individual lambs of each genotype. B) Fold change between the group mean gene expression ($\log_{10}$ axis) for heterozygous ($^{+/-}$) vs. homozygous ($^{-/-}$) mutant testes. The baseline (no difference) is indicated with a horizontal dashed line. The 95% CIs represent the uncertainty around the estimated coefficients for the fixed effect of genotype in a linear mixed-effects model, which includes different animals as random effects. C) Hematoxylin and eosin-stained (H&E) sections of neonate lamb testis (top row). Magnified areas (stippled boxes) show putative prospermatogonia (inset, yellow arrow heads) in the lumen of *NANOS2*$^{+/+}$ and *NANOS2*$^{+/-}$ but not *NANOS2*$^{-/-}$ testis cords. Immunostaining of germ cell (DDX4 and SSEA4) and somatic (GATA4, SOX9, ACTIN, and 3β-HSD) markers in neonate testis cryosections (middle rows). Spermatozoa and azoospermia in adult ejaculates (bottom row). Scale bars = 50 µm.

Table 2. Reproductive phenotype of male *NANOS2* clones.

NANOS2[a]	Sire ID	Sperm quality			IVF					Artificial insemination		Natural mating	
		% alive fresh	Motility[b]	% alive postthaw	*n*[c]	nIVC[d]	>1-cell (%)	M/B (%)[a–c,e]	M/B (%)[a–b,f]	No. of ewes	No. of lambs	No. of ewes	No. of lambs
–/–	1812	Nil	—	—	—	—	—	—	—	—	—	—	—
+/–	1945	70	3.5	45	2	80	71 (89)	28 (35)	10 (13)	5	7	2	4
+/+	1942	75	3	42	2	80	70 (88)	25 (31)	8 (10)	ND[g]	ND[g]	1	2

[a]Sperm genotype.
[b]Motility scale 1–5 (low-high).
[c]Number of replicates.
[d]Number of embryos placed into in vitro culture (nIVC).
[e]nIVC that developed into compact morula (M) or blastocysts (B) of morphological grades 1–3 (M/Ba–c).
[f]M/B of morphological grades 1 and 2 (M/Ba–c).
[g]Not determined.

Table 3. Oocyte recovery from female *NANOS2* clones.

NANOS2[a]	Ewe ID	nOPU[b]	No. of follicles	No of oocytes	Follicles/donor	Oocytes/donor	Oocytes/follicle
–/–	1927	4	53	52	13.3	13.0	1.0
–/–	1938	4	47	26	11.8	6.5	0.6
–/–	1936	1	12	11	12.0	11.0	0.9
–/–	Subtotal	9	112	89	12.4	9.9	0.8
+/+	1935	4	47	49	11.8	12.3	1.0
+/+	1928	4	41	38	10.3	9.5	0.9
+/+	1930	4	47	34	11.8	8.5	0.7
+/+	1941	2	31	32	15.5	16.0	1.0
+/+	Subtotal	14	166	153	11.9	10.9	0.9

[a]Oocyte genotype.
[b]Number of OPU sessions.

Table 4. OPU-IVP with gametes from *NANOS2* clones.

NANOS2[a]		IVF				
Sperm	Oocyte	*n*[b]	nIVC[c]	>1-cell (%)	M/B (%)[a–d]	M/B (%)[a,b,e]
–/+	–/–	2	32	11 (97)	10 (31)	4 (13)
–/+	+/+	2	57	51 (89)	24 (42)	16 (28)

[a]Gamete genotype.
[b]Number of replicates.
[c]Number of embryos placed into in vitro culture (nIVC).
[d]nIVC that developed into compact morula (M) or blastocysts (B) of morphological grades 1–3 ($M/B^{1–3}$).
[e]M/B of morphological grades 1 and 2 ($M/B^{1–2}$).

respectively, Fig. 4B). This indicates the germline was complemented in the chimeric fetus. For the nontransgenic Texel donors, 12 putative chimeric lambs were produced at term, only one of which survived beyond weaning. The only surviving lamb (1942) developed into adulthood with a distinct Texel phenotype. Following successful natural mating, which resulted in only wild-type offspring, the animal was euthanized for welfare reasons. Postmortem ddPCR revealed only wild-type and no mutant allele contribution in brain, kidney, liver, and testis. We conclude that this animal was nonchimeric and exclusively derived from the Texel donor cells.

PCR analysis of the 11 deceased neonates for both the mutant and wild-type *NANOS2* alleles confirmed that all lambs were chimeric in at least one tissue. The level of chimerism was variable and ranged from extremely low (<0.1% in L24, L28, L29, L34, and L35) to low (L26, L27, L30, and L31) to balanced (L32 and L33) contribution of both aggregation partners (Fig. 4C, D). The number of prespermatogonia was quantified in the same samples (Fig. 4E). Those lambs that were identified as chimeric by PCR showed various degrees of germline colonization, ranging from nil (L24, L28, L30, and L35) to medium (L27, L31, and L33) and to wild-type levels (L29, L32, and L34). Extremely imbalanced chimeras with mostly mutant (L24, L28, and L35) or wild-type (L29 and L34) alleles contained either no prospermatogonia or numbers fell within the normal range of wild-type Texel rams (L15 and L17), respectively. Representative hematoxylin and eosin (H&E) testis sections from all lambs analyzed show comparable tissue preservation, except for two samples (L26 and L30) with poorer morphology (Fig. S5a). In fact, one of these samples (L26) contained DDX4-positive prospermatogonia, indicating that it was a chimera, consistent with its PCR results (Fig. S5b). In summary, it was possible to produce germline chimeras with fully restored prospermatogonia numbers for absolute transmission of the donor cell genotype.

Discussion

We introduced biallelic mutations in the *NANOS2* gene, ablating the germline in cloned rams but not affecting female reproductive performance. The vacant testis niche was filled by morula complementation, producing chimeric lambs with partially to fully restored germ cell numbers. Together with the demonstration that heterozygous *NANOS2* rams are fertile, this provides an absolute transmitter breeding platform to accelerate genetic improvement of livestock.

NANOS2 phenotype

Neonatal *NANOS2*$^{-/-}$ lamb testis lacked prospermatogonia, which was inferred from analyzing mutant testis samples for gene expression and histology. Based on ellipsoid testis geometry and

Table 5. Breeding *NANOS2* F1 offspring by OPU-IVP.

NANOS2[a]		Recipients		Offspring						Live *NANOS2* lambs[b]		
Sperm	Oocyte	nET[c]	No. of recipients	Born	Live	Dead	Survival/ET (%)	Survival/ewe (%)	Survival/born (%)	−/−	−/+	+/+
−/+	−/−	11	4	3	2	1	27	50	67	1	1	0
−/+	+/+	25	8	8	5	3	20	63	63	0	2	3

[a]Gamete genotype.
[b]*NANOS2* genotype of offspring.
[c]Number of embryos transferred (nET).

dimensions, we estimate that these techniques surveyed ~0.3% (~3 mm^3) and ~8% (~81 mm^3) of the neonatal sheep testis, respectively. Mutant testis parenchyma showed up to 5,000-fold reduced average expression of germ cell markers (*DAZL*, *LIN28*, and *NANOG*) compared with wild type. *NANOS2* and *DDX4* remained detectable but were reduced by one to two orders of magnitude, respectively. Thus, we cannot rule out that residual prospermatogonia are still present, even though they were not identified by histological examination. Residual expression may be due to incomplete clearance of apoptotic germ cells. Alternatively, somatic cells may add biological noise by sporadically producing low, nonfunctional levels of germline transcripts, as observed in human testis (24, 25).

We neither saw morphologically identifiable germ cell nuclei nor positive immunostaining for DDX4 or SSEA4. Conclusively, the ejaculate of sexually mature *NANOS2*$^{-/-}$ rams did not contain spermatozoa, extending findings in mice, pigs, and goats (10–15). In mice, *Nanos2* is required for sexual differentiation of germ cells and maintaining mitotic arrest (26). Germ cells lacking *Nanos2* apoptosis, with their numbers approximately halved compared with heterozygous controls before birth, and none seen after puberty (17). A similar phenotype was found after the onset of puberty in pigs (10, 12) and goats (10). Sheep female germ cells enter meiosis around 55 days postconception (27), but the timing of spermatogonial specification and onset of *NANOS2* expression is unknown in this species. The interval between *NANOS2*-mediated lineage specification and birth is longer than in mice, extending the time for eliminating germ cells and perhaps explaining the already complete loss of germ cells in neonates, similar to earlier germ cell loss observed in *DAZL*-null sheep (14). A *NANOS2*$^{-/-}$ fetal bull calf at 253 days of gestation also showed no DDX4-positive germ cells in the testicular parenchyma (10).

On the contrary, the somatic testis compartment in *NANOS2*$^{-/-}$ lambs was unchanged with regard to marker proteins and transcripts for Sertoli (28), Leydig (29), and peritubular myoid cells (30). This is consistent with *NANOS2* ablation in other mammals, which showed the somatic cells of the testis were intact (10), testosterone production normal (12), and able to initiate spermatogenesis after transplantation of exogenous spermatogonial stems cells (10).

Chimera production by morula aggregation

Previous livestock chimeras were produced by transplanting donor cells around the eight-cell stage, analogous to the procedure frequently used in mice. However, we demonstrate that aggregating compacted morulae was more efficient for producing chimeric blastocysts and animals for several reasons. First, embryonic genome activation (EGA) occurs at the two-cell stage in mice but at the eight-cell stage in sheep and cattle (31). Failure to correctly initiate EGA will halt development, with 50–80% of murine embryos arresting at the two-cell (32) stage. Therefore, mouse eight cells have already progressed post-EGA and are more developmentally competent than livestock eight cells. Delaying aggregation until the 32-cell stage in sheep, equivalent to the eight-cell stage in mouse, maximizes the developmental potential of each aggregation partner to contribute to a chimeric blastocyst. Second, zona-free sheep compacted morulae are easily identified through their distinct morphology and adherence to the substrate. By contrast, precompacting cleavage stages often fragment into small, regular-sized anuclear cells that can be mistaken for intact, later-stage blastomeres. Third, compacted morula aggregation does not compromise subsequent cell mixing in chimeras. Following eight-cell aggregation and live tracking in mouse, cell movements within the inner cell mass led to extensive cell mixing in adult tissues (33). Similarly, clonal injection of epiblast cells into blastocysts showed complete intermingling in the pre-gastrulating epiblast (34). Fourth, aggregating compacted morula was less time-consuming and labor-intensive, with ~4-fold fewer embryos needed for selection, dissociation, and aggregation compared with 8–32 cells. Fifth, morula aggregation does not require specialized micromanipulation equipment, training, and skill (35). Collectively, aggregating compacted morulae is a successful strategy for producing sheep chimeras.

Embryonic germline complementation

Since *NANOS2*$^{-/-}$ lambs have no detectable prospermatogonia at birth, we infer that in the chimeric lambs all germ cells derived from the donor. To strengthen this conclusion, we attempted co-localization of *mCherry* and DDX4 protein or mRNA by immunofluorescence or in situ PCR, respectively, but the autolyzed lamb tissue was too degraded for both approaches. Alternatively, it may be possible to demonstrate that all prospermatogonia were *NANOS2*$^{+/+}$ by employing spatial multiomics with DNA or germ cell-specific mRNA probes that differentiate between donor (Texel) vs. host (composite/Perendale) cells (36). Since none of the chimeric lambs survived to puberty, it was not possible to verify the genetic donor origin of the donor sperm from ejaculates. Previous reports of germline complementation in livestock using *NANOS3*$^{-/-}$ female cattle had the same limitation (11).

All but one of the 13 lambs born were chimeric in at least one tissue. The only nonchimeric lamb, which was exclusively derived from the Texel donor, was the sole survivor to puberty. Since all lambs were derived from aggregating cloned embryos, their poor in vivo development can be attributed to the cloning syndrome. This is particularly problematic in sheep where only ~30% of animals born survive to weaning (37). In our hands, sheep cloning efficiency after embryo complementation was 15% (38), similar to the term efficiency in putative clone chimeras (13/96 = 14%). The perinatal pathologies were consistent with the spectrum of cloning-related phenotypes (37).

The level of chimerism ranged from extremely low to low to balanced contribution of both aggregation partners (46 to 31 to 23%,

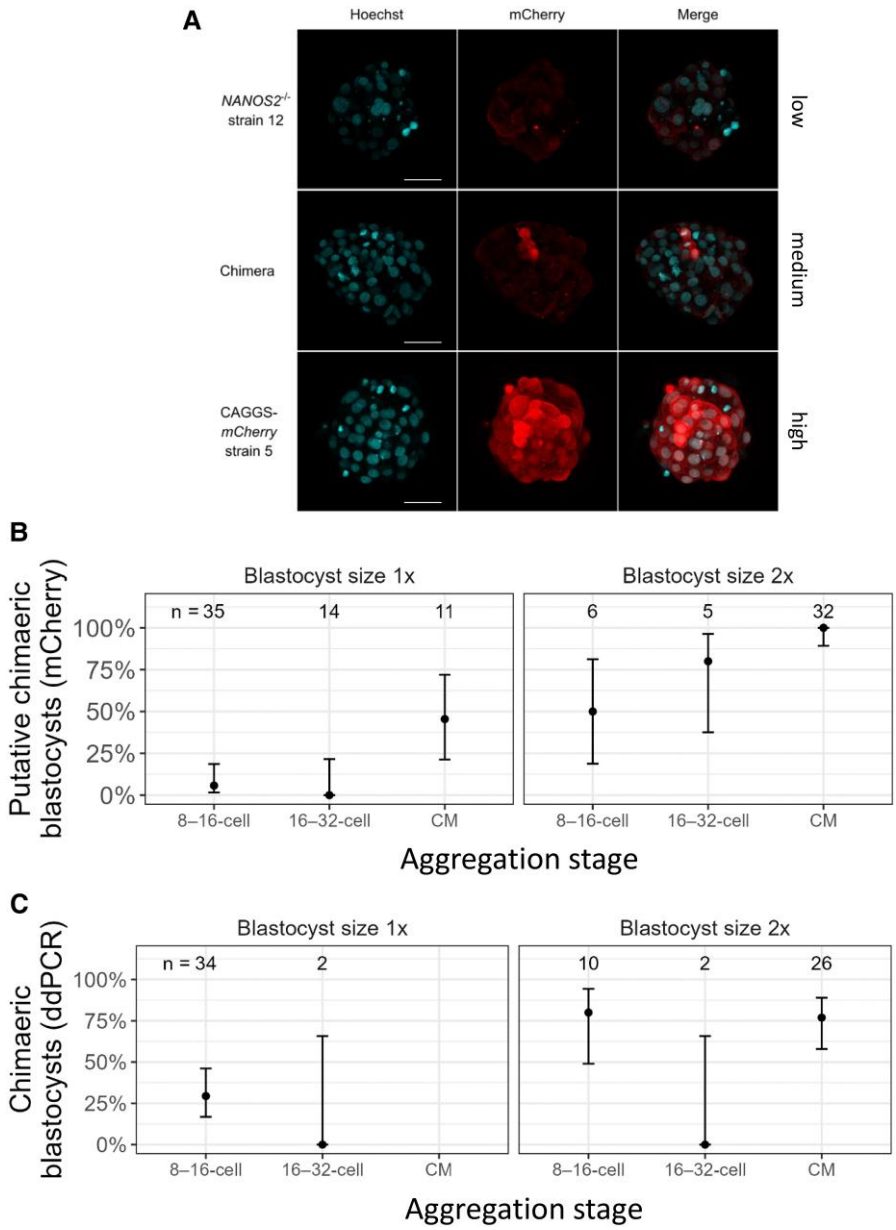

Fig. 3. Determining chimerism in blastocysts and lambs. A) Observed chimerism in aggregation blastocysts (middle panel) compared with *NANOS2*$^{-/-}$ blastocysts (cell strain #12, top panel) and mCherry blastocysts (cell strain #5, bottom panel). Images are confocal maximum intensity projections. DNA was stained with Hoechst 33342. Scale bar = 50 µm. B, C) Following aggregation of mCherry donor and *NANOS2*$^{-/-}$ host embryos at the 8–16-cell, 16–32-cell, or compacted morula (CM) stage, blastocysts were sized as normal (1×) or enlarged, indicative of successful aggregation (2×). Chimerism was determined by subjective classification of live mCherry signal from epifluorescence observation (b) and ddPCR of the *NANOS2* wild-type allele, normalized on reference gene *CSN2* copies (c). Shown are the 95% CIs for the proportion using the Wilson's score method (*n*, number of blastocysts analyzed).

respectively, of lambs born). Most of the lambs categorized as extremely low or low chimeras either showed no germline colonization or normal numbers of presumably wild-type sperm. The best candidates for absolute germline transmitters were six lambs with low to balanced chimerism containing low to normal numbers of prospermatogonia (L4, L26, L27, L31, L32, and L33). Another lamb with low chimerism (L30) showed very poor tissue preservation, which compromised reliable detection of prospermatogonia. While we generated at least 6/13 = 46% potential transmitter rams, their fertility remains unproven. In mouse, embryo complementation of genetically sterilized male hosts produced over 50% of chimeras, but not all transmitted their germline, resulting in ~20% fertile absolute transmitters (7, 15). This benchmarks what efficiencies might be expected for livestock embryo complementation. Embryo-complemented animals must produce physiological amounts of sperm when they reach puberty. In mouse, spermatogenesis follows a normal spatiotemporal pattern with normal numbers of offspring being routinely produced at puberty (7). Even though quantitative sperm output still requires more detailed investigation, this method has been used for decades to produce genetically modified (GM) mice.

Sourcing of embryonic donors is minimally invasive due to the widespread use of embryo IVP systems, allowing routine access to embryos from high genetic value donors. While blastomere numbers are limited, ESCs can extensively expand in vitro, even after complex genome modifications (39). Livestock ESCs have become available in pigs (22), sheep (40), and cattle (23, 41). Future production of absolute transmitters by embryo complementation

Table 6. Chimerization efficiency.

Aggregation day	n[a]	Aggregated embryos[b]	Aggregation blastocysts (%)[c]	Chimeric blastocysts (%)[d]
3	4	136	41 (30)[a]	5 (4)[a]
4	1	30	19 (63)[b]	4 (13)[a]
5	5	38	43 (113)[c]	37 (97)[b]

[a]Number of replicates.
[b]Number of aggregated host *NANOS2*$^{-/-}$ (strain 12 or 33) and donor *mCherry* (strain 5 or 9) embryos.
[c]Number of blastocysts after aggregation.
[d]Number of chimeric blastocysts after scoring red fluorescence and size (medium and 2×, respectively).
[abc]Rows with different superscripts differ $P < 0.005$, Fisher's exact test.

critically relies on livestock ESCs and germline-deficient hosts provide an experimental test system to assess their germline competency.

Applications for germline chimeras

Germline complementation in sheep offers a new route for multiplying valuable embryonic cells into germline transmitters that disseminate high-value sperm by AI or natural mating (42). There are potential benefits of this approach for agriculture, biomedicine, and species conservation.

For agriculture, elite genotypes are increasingly selected from biopsies of IVP embryos (42). However, less than half of IVP embryos generate live offspring (43); the remainder of potentially elite genetic combinations is lost from the breeding population. Such genetic wastage could be reduced by splitting elite embryos or converting them into ESCs before complementing germline-depleted hosts. This would multiply their germline across numerous chimeric blastocysts to increase the chances of producing offspring. To produce enough host embryos, *NANOS2*$^{+/-}$ sperm can be used to fertilize *NANOS2*$^{-/-}$ oocytes, producing 25% sterile male$^{-/-}$ embryos (or 50% when using sex-sorted male sperm for IVF). Embryo-based genomic selection ties in seamlessly with embryo complementation. Both could be combined with gene editing donor cells to assemble high-impact causative sequence variants in individual genomes in a single generation, which is impractical with conventional breeding strategies (42). This will allow the technology to transition from short-term clone↔clone chimeras, as described in this proof-of-principle study, to long-term IVP↔IVP chimeras with projected better animal survival. From a regulatory perspective, absolute transmitters are "null segregants" who cannot transmit the knockout mutation, which defined their parents as GM. In extensively farmed livestock, large transmitter teams would provide a superior alternative to AI by widely disseminating high-value, non-GM sperm through natural mating, for faster introgression of desirable traits.

For species conservation, germline-ablated, domestic hosts would provide embryos for complementation with donor cells from closely related endangered (or even extinct) species. Interspecies chimeras have produced live offspring in laboratory rodents (6). Alternatively, cloned blastomeres or ESCs from endangered species could be used for complementation. Due to their IVP component, chimeric IVP↔cloned embryos are expected to survive better into adulthood than cloned embryos (44).

Improved survival would also be beneficial for agrimedical applications, generating gene-edited livestock for human disease modeling, therapy, and determination of gene function (45). Embryo complementation would allow propagation of severe disease phenotypes or embryonic lethal mutations and analysis of their germ cell function in founder animals (15). Thus, efficient embryonic germline colonization can enable a novel molecular breeding platform that integrates embryo complementation with embryo-based genomic selection, genome modification, and multiplication, capturing the most recent genetic gains as absolute germline chimeras.

Materials and methods

All animal studies were undertaken in compliance with the New Zealand Animal Welfare Act and were approved by the Ruakura Animal Ethics Committee (approval numbers 13801, 13802, 14257, 14395, 14396, 14696, 14697, 15051, 15064, and 15067).

Cell derivation

MFFs and FFFs, previously known as OFF3 and PDFF3, respectively, as well as adult ear skin fibroblasts from an elite short-tailed Texel ram (previously known as Texel adult ear fibroblasts) were derived as described (38).

Genome editing

Several gRNAs were identified within the target region for *NANOS2* (NCBI gene ID: 101115150) and selected for minimal off-target sites using CCTop (46). An asymmetric oligonucleotide with 36- and 91-bp homology arms was used to increase HDR efficiency (47). Editing and ddPCR detection were carried out as described with normalization on a *Beta-casein* (*CSN2*) genomic reference HEX-labeled hydrolysis probe (14). Edited cell strains were obtained by manually selecting mitotic cells, followed by ddPCR screening, Sanger sequencing, and TIDE analysis (48) as described (14). For confirmation of heterozygosity and to ensure clonality, SCT into bovine oocytes was performed (see below). Genomic DNA was extracted from 25 SCT embryos at the 8–32-cell stage and Sanger sequencing confirmed all as heterozygous. Genomic DNA samples were screened for gRNA–Cas9 plasmid insertion by Sanger sequencing of PCR-amplified fragments (Table S4) and whole-genome sequencing.

Off-target analysis

Different genotypes were sequenced via DNBseq (BGI, Hong Kong). The samples included (i) nonedited MFFs, (ii) nonedited FFFs (1941), (iii) a NANOS2$^{+/-}$ male lamb (1945), and (vi) 3 NANOS2$^{-/-}$ female lambs (1927, 1936, and 1938). Between 565 million and 1.4 billion reads per library gave a 32- to 80-fold coverage of the ovine genome. Reads were mapped to the ARS-UI_Ramb_v3.0 reference genome (GCF_016772045.2) using bwa mem (v0.7.17) with soft clipping for supplementary alignments (-Y) (49). Alignments were converted into binary alignment (BAM) format using samtools (version 1.13) (50) and processed with GATK MarkDuplicates (v4.5.0.0) to flag PCR- and optical-duplicate reads. Variants were called using bcftools mpileup (v1.19) (51), GATK HaplotypeCaller (v4.5.0.0) (52), and freebayes (v1.3.8, https://github.com/freebayes/freebayes). To calculate the expected depth, the negative binomial quantile function in R was used to obtain the 0.001 and 0.999 quantiles. We also added depth filtering for raw variant calls at the cohort level (MFF vs. FFF) and allele calls for the SNPs unique to each individual lamb. Variants were filtered to remove (i) monomorphic variants, (ii) variants with all-sample read raw depth limits of <33 and >103/<119 and >234 and unique variant depth limits of <12 and >61/<19 and >76 or MFF/FFF, respectively, and (iii) natural variation present in the European Variant Archive (v6) (https://doi.org/10.1093/nar/gkab960) for *O. aries*. The intersection of the

Table 7. Generating clone↔clone chimeras.

Clone ↔ clone offspring					Chimeric		Nonchimeric	
Donor genotype	Aggregation day	nET	No. of lambs (%)	No. of adults (%)	ddPCR[a]	Germ cells[b]	Host *NANOS2*$^{-/-}$ (%)	Donor WT (%)
Composite_mCherry	3	16	3 (19)[c]	0	0 (0)	0 (0)	3 (100)	0 (0)
Composite_mCherry	4	10	0	0	—	—	—	—
Composite_mCherry	5	22[d]	1 (5)[e]	0 (0)	1 (100)	1 (100)	0 (0)	0 (0)
Composite_mCherry[f]	—	17	0	0	—	—	—	—
Texel	5	74	12 (16)	1 (7)	11 (92)	6 (55)	0 (0)	1 (8)
Texel[f]	—	22	4 (18)	0 (0)	0 (0)	0 (0)	0 (0)	2 (100)[g]

[a]Tissues analyzed by ddPCR with *NANOS2* WT vs. MUT hydrolysis probes: brain, kidney, liver, and testis.
[b]Prospermatogonia were quantified on H&E-stained paraffin sections of neonate testis.
[c]One lamb terminated on day 114 due to hydroallantois.
[d]Eight blastocysts were degenerating before embryo transfer.
[e]One lamb aborted on day 133.
[f]Nonaggregated control.
[g]Only two out of four lambs born were analyzed (L15 and L17).

resultant variants from all three variant callers was further analyzed (https://github.com/BenjaminJPerry/SMK-SNVS/tree/aihoove). Potential off-target sites were found using fuzznuc (version 6.6.0.0) and CRISPOR (version 4.98) by searching for each CRISPR target sequence with up to five mismatches (53, 54), extending 100 bp from either end of the gRNA-binding site. Potential off-target sites were converted into a BED file containing (i) chromosome, (ii) potential off-target start, and (iii) potential off-target end coordinate. The vcf file was filtered for variants overlapping the potential off-target (BCFtools v1.19). Variants overlapping potential off-target sites that had different genotype calls between the wild-type and edited samples were manually inspected using IGV (version 2.8.2) (55). Manual inspection consisted of checking for soft-masked (lower case) and repetitive sequence and nucleotide quality (q30) at the affected site. Homozygous large deletions and insertions at potential off-target sites were evaluated. The depth command of SAMtools (v1.13) (50) with the read and nucleotide qualities both set to 30 was used to calculate the depth of each position at the potential off-target sites. Average sequencing depth of each site was calculated using Microsoft Excel and filtered with zero reads as a cutoff. No regions with zero reads were observed in any samples, indicating that there were no large indels.

mCherry transgenesis

The reporter plasmid, expressing mCherry from a CAGGS promoter (56), was modified to include a puromycin resistance gene driven by a constitutive PGK promotor. The PGK-PuroR/CAGGS-mCherry plasmid and hyperactive *Sleeping Beauty* transposase (pCMV-SB100X) (56) were transfected into MFFs, puromycin-selected, and colonies isolated using cloning cylinders (Sigma, USA). A FACSVerse flow cytometer (BD Biosciences, USA) was used following the manufacturer's instructions.

Copy number variation (CNV) was quantified on the QX200 (Bio-Rad) ddPCR system with primer/fluorescent hydrolysis probe mixes for *mCherry* (6-FAM) and beta-casein (*BCSN2*) reference (VIC), respectively (Table S4). Primer/probe pairs were designed with Primer3Plus, and the template DNA was digested with *HindIII*. The following program was used: (i) denature (30 s at 95 °C); (ii) amplify (10 min activate at 95 °C, 30 s denature at 94 °C, 60 s anneal/extend at 60 °C for 40 cycles); and (iii) melting curve (95 °C, cooling to 70 °C, heating at 0.1 °C/s to 95 °C while measuring fluorescence).

SCT cloning and embryo complementation

SCT with G_0 cells was carried out based on a modified zona-free cloning protocol (57). Briefly, MII oocytes were enucleated 19 h postmaturation (hpm). Caffeine (5 mM) was included in the medium from 20.5 to 26.5 hpm (38). Activation by ionomycin/6-dimethylaminopurine was carried out ~27 hpm. Groups of 10 embryos were cultured in 20 µL drops of SOFaaBSA, each embryo occupying a manually prepared microwell. After 3–5 days, embryos with regular morphology were disaggregated (HEPES-buffered SOF without calcium and BSA, containing 0.1 mg/mL PVA, 0.2 g/mL EDTA, 5 µg/mL cytochalasin-B) for 2 min by blowing up and down with a pipette (an inner diameter of 50–70 µm). Disaggregated embryos of similar developmental stage were combined by repeated pipetting inside a mouth pipette and placed in a microwell to compact into a single morula. After 5–6 h, morulae were transferred into a fresh culture drop. Blastocysts were morphologically graded (58) and either vitrified or transferred into recipient ewes. Pregnancies were monitored by ultrasound throughout gestation and hormonally inducted (59).

Gene expression analysis

Snap-frozen testis parenchyma was homogenized in TRIzol, RNA extracted, and DNA removed with DNase I following the manufacturer's instructions. A "no reverse transcription" control was included. cDNA was synthesized using SuperScript IV according to the manufacturer's instructions. KAPA SYBR FAST qPCR Kit (Kapa Biosystems) was used with a MIC qPCR Cycler (Bio Molecular Systems) using running conditions and normalization on the geometric mean of *GAPDH*, *HPRT*, and *ACT* (14). Expression of other candidate markers was validated in wild-type testis by confirming (i) amplification of a single product through gel electrophoresis and melt analysis and (ii) dynamic range over four orders of magnitude by serial dilution. Only intron-spanning primer pairs that passed these quality controls were analyzed (Table S5). When amplicons were not detected, an arbitrary baseline with a C_q of 35 was set.

Histology and immunofluorescence

Neonate gonads were fixed in Davidson's solution for paraffin sections or in 4% paraformaldehyde (PFA) for frozen sections. Hematoxylin–eosin-stained paraffin sections were analyzed by a pathologist service (Veterinary Pathology Ltd, Hamilton, New Zealand). Prospermatogonia were counted from 15 random fields of view per animal and normalized on testis cord area. Follicle numbers were counted by a pathologist. Lamb identity was masked for quantification. PFA-fixed testes were washed through 30% (w/v) sucrose, frozen in OCT compound, and sectioned at 8 µm using (Leica CM1850 cryostat). Sections were immunostained

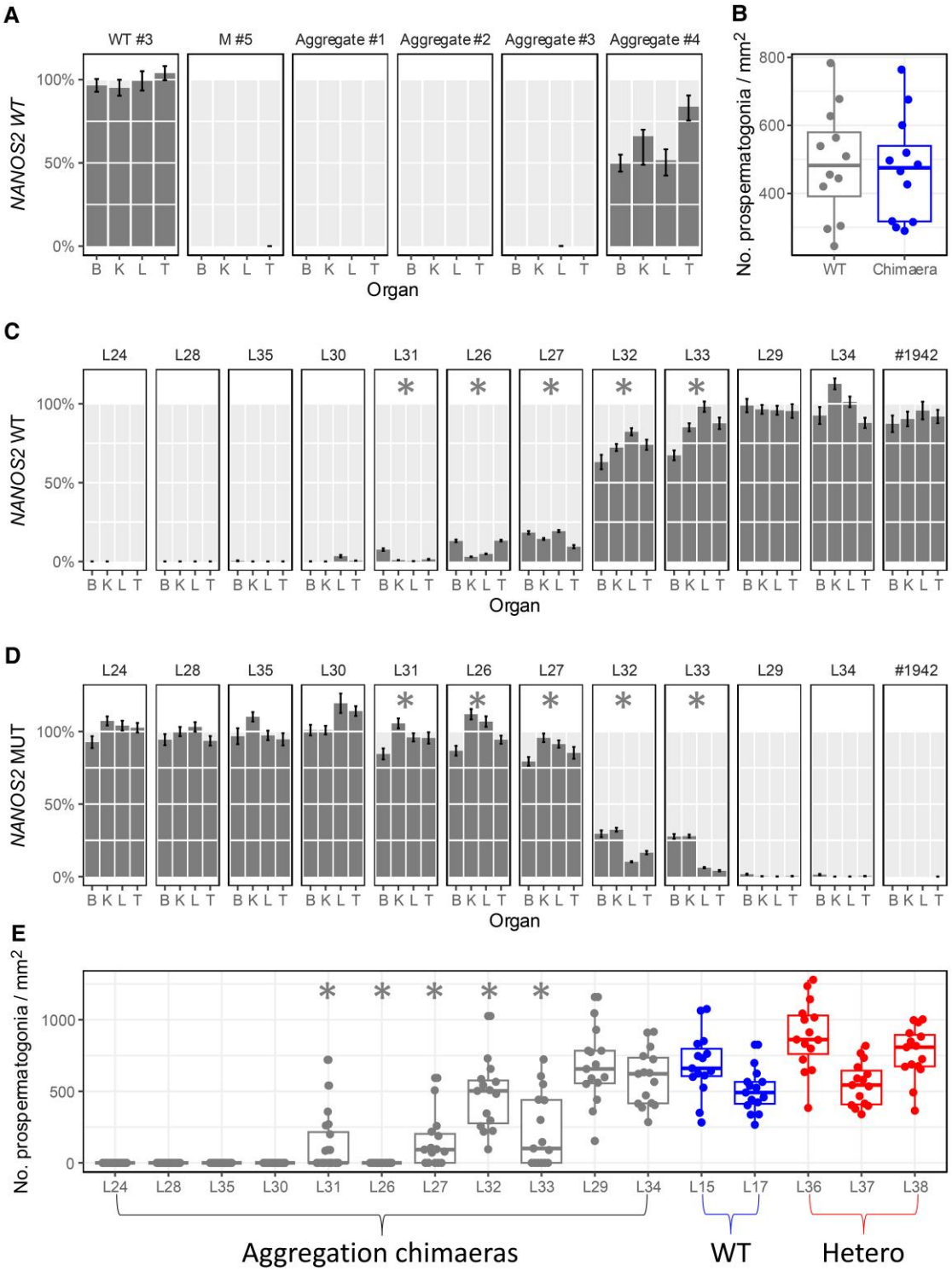

Fig. 4. Germline complementation in chimeric lambs. Following aggregation of elite wild-type (WT) donor and *NANOS2*$^{-/-}$ host embryos at the compacted morula stage, blastocysts were transferred into gestational surrogates. A) Chimerism was quantified by ddPCR of the *NANOS2* WT allele in representative organs (B = brain, K = kidney, L = liver, T = testis) of deceased lambs, including WT (#3) and mutant (M #5) control lambs, normalized on reference gene *CSN2* copies. Aggregate lambs #1–3 were from 8–16-cell aggregation and predicted to be nonchimeric (1×) at the blastocyst stage; aggregate lamb #4 was from a CM aggregation and predicted to be chimeric (2×). For ddPCR results, black vertical bars show the 95% CI from the technical Poisson error. (B) Prospermatogonia were counted in H&E-stained testis sections from the chimeric lamb (L4) and an age-matched WT lamb. Counts were normalized on the testis cord area (mm^2). C) Chimerism was quantified by ddPCR of the *NANOS2* WT and D) mutant (MUT) allele in representative organs of 11 deceased putative chimera neonates. E) Prospermatogonia were counted in H&E-stained testis sections from nine putative chimeric lambs, two WT, and one heterozygous mutant control lambs. Counts were normalized on the testis cord area (mm^2). Asterisks mark putative chimeras.

with primary antibodies 1:100 anti-DDX4 (ab13840, Abcam), 1:50 anti-SSEA4 (sc-21704, Santa Cruz Biotechnology), 1:300 anti-SOX9 (AB5535, Merck Millipore), and 1:50 anti-3β-HSD (sc-100466, Santa Cruz Biotechnology) as described (14). Primary antibodies were labeled with corresponding Alexa Fluor secondary antibodies (A-11036, Ab150073, A-10037, Thermo Fisher Scientific) and

costained with Hoechst 33258 and 1:1,000 Phalloidin-iFluor 488 (ab176753, Abcam). Images were taken with an epifluorescence Olympus AX70 microscope and processed with ImageJ (version 1.45s) for identical brightness adjustment and colourization of wild-type and mutant samples.

Chimera analysis

The degree of chimerism was noninvasively estimated by (i) the size of the blastocyst and (ii) the presence and distribution of mCherry signal. Size was categorized as 1× (normal) or 2× (larger than normal), with a focus on ICM, rather than blastocoel size. Incorporation of blastomeres after aggregation was also considered, with 1× containing developmentally arrested, extruded blastomeres, and 2× having most blastomeres integrated into the embryo. The mCherry signal was assessed by fluorescence illumination and categorized as "low," if all blastomeres appeared nonfluorescent; "medium," if both mCherry-positive and negative blastomeres were identified; or "high," if only mCherry signal was detectable. Putative chimeric blastocysts by mCherry signal were then defined as embryos with "medium" scored signal.

Subjective categorization was validated by ddPCR on extracted DNA using hydrolysis probes specific for the wild-type and mutant alleles (Table S4). Individual blastocysts were lysed in 1× PCR buffer (Thermo Fisher, New Zealand) and 1 mg/mL proteinase K with a 55 °C incubation for 30 min, followed by a 95 °C inactivation for 10 min. Using 2 µL of the sample, the *NANOS2* region was preamplified for 10 cycles. For ddPCR, the manufacturer's instructions were followed using 2 µL of the preamplified product. Embryos were categorized as nonchimeric if they were composed entirely of a single genotype and chimeric if they were not. To detect chimerism in animals, snap-frozen tissue was digested in proteinase K overnight at 55 °C and genomic DNA isolated by phenol/chloroform extraction. Relative contribution of wild-type *NANOS2* was quantified by ddPCR as above.

Breeding

Ejaculates and oocytes were collected from edited and nonedited adult rams and ewes, respectively, following commercial protocols (Animal Breeding Services Ltd, New Zealand). Sperm quality was assessed using commercial live sperm parameters before and after freezing (Animal Breeding Services Ltd). Rams were naturally mated, or their sperm used for AI.

Statistics

Following statistical best practice, we display 95% CIs where possible and detailed in the legends. For developmental data (Tables 1–7), *P*-values were determined using the Fisher's exact test in 2 × 2 tables.

Acknowledgments

The authors thank Wilfried Kues for donating the CAGGS-mCherry and SB100× plasmids, Stefan Wagner for CSN2 probe, Alan Julian for histological services, Stephanie Delaney for animal husbandry, and Elyssa Barnaby for veterinarian care. Expression vector pSpCas9(BB)-2A-Puro (PX459) V2.0 was a gift from Feng Zhang (Addgene plasmid 62988). The PGK-PuroR plasmid was a gift from Rudolf Jaenisch (Addgene plasmid 11349) with a polyA signal modification by Goetz Laible.

Supplementary Material

Supplementary material is available at *PNAS Nexus* online.

Funding

Z.L.M. was partially supported by a Livestock Improvement Corporation fellowship grant. S.J.A. was supported by a University of Auckland Doctoral Scholarship and Todd Foundation Award for Excellence. This study was supported by funds from the Ministry of Business, Innovation and Employment (C10X1711), AgResearch and the University of Auckland.

Author Contributions

Z.L.M., L.M.F., and B.O. conceived and designed the experiments. Z.L.M. and L.M.F. carried out most of the experiments, processed and analyzed the data, and produced the figures. S.J.A. contributed to sheep cloning, while J.W., D.N.W., and F.M. enucleated oocytes, and J.W. vitrified blastocysts. B.B. performed some ddPCR analysis. P.H.M. and B.J.P. undertook off-target bioinformatics from WGS data. P.T. contributed to sheep cloning, mCherry qPCR, and CNV analysis. B.F.-G. helped with histology and IF data acquisition. Z.L.M., L.M.F., and B.O. wrote the manuscript with input from D.N.W. and R.G.S. All authors read and provided comments and approved the final manuscript.

Data Availability

Whole-genome sequencing data were deposited in the NCBI (ID 1213111—BioProject—NCBI). All mapping, alignment, and variant filtering analysis is available through GitHub (https://github.com/BenjaminJPerry/SMK-SNVS/tree/ai-hoove). The authors confirm that all data supporting the findings of this study are available within the article and its supplementary materials.

References

1 Mueller ML, Van Eenennaam AL. 2022. Synergistic power of genomic selection, assisted reproductive technologies, and gene editing to drive genetic improvement of cattle. *CABI Agric Biosci.* 3:1–29.
2 Spanner EA, de Graaf SP, Rickard JP. 2024. Factors affecting the success of laparoscopic artificial insemination in sheep. *Anim Reprod Sci.* 264:107453.
3 Rexroad C, *et al.* 2019. Genome to phenome: improving animal health, production, and well-being—a new USDA blueprint for animal genome research 2018–2027. *Front Genet.* 10:327.
4 Oback B, Cossey DA. 2023. Chimaeras, complementation, and controlling the male germline. *Trends Biotechnol.* 41:1237–1247.
5 Zhang X, *et al.* 2021. Establishment of Etv5 gene knockout mice as a recipient model for spermatogonial stem cell transplantation. *Biol Open.* 10:bio056804.
6 Kobayashi T, *et al.* 2021. Blastocyst complementation using Prdm14-deficient rats enables efficient germline transmission and generation of functional mouse spermatids in rats. *Nat Commun.* 12:1328.
7 Koentgen F, *et al.* 2016. Exclusive transmission of the embryonic stem cell-derived genome through the mouse germline. *Genesis.* 54:326–333.
8 Zvick J, *et al.* 2022. Exclusive generation of rat spermatozoa in sterile mice utilizing blastocyst complementation with pluripotent stem cells. *Stem Cell Reports.* 17:1942–1958.
9 Zhou H, Zeng Z, Koentgen F, Khan M, Mombaerts P. 2019. The testicular soma of Tsc22d3 knockout mice supports spermatogenesis and germline transmission from spermatogonial stem cell lines upon transplantation. *Genesis.* 57:e23295.

10 Ciccarelli M, *et al.* 2020. Donor-derived spermatogenesis following stem cell transplantation in sterile NANOS2 knockout males. *Proc Natl Acad Sci U S A*. 117:24195–24204.
11 Ideta A, *et al.* 2016. Generation of exogenous germ cells in the ovaries of sterile NANOS3-null beef cattle. *Sci Rep*. 6:24983.
12 Park K-E, *et al.* 2017. Generation of germline ablated male pigs by CRISPR/Cas9 editing of the NANOS2 gene. *Sci Rep*. 7:40176.
13 Speed R, Taggart M, Cooke H. 2003. Spermatogenesis in testes of Dazl null mice after transplantation of wild-type germ cells. *Reproduction*. 126:599–604.
14 McLean ZL, Appleby SJ, Wei J, Snell RG, Oback B. 2021. Testes of DAZL null neonatal sheep lack prospermatogonia but maintain normal somatic cell morphology and marker expression. *Mol Reprod Dev*. 88:3–14.
15 Miura K, Matoba S, Hirose M, Ogura A. 2021. Generation of chimeric mice with spermatozoa fully derived from embryonic stem cells using a triple-target CRISPR method for Nanos3. *Biol Reprod*. 104:223–233.
16 Suzuki A, Saga Y. 2008. Nanos2 suppresses meiosis and promotes male germ cell differentiation. *Genes Dev*. 22:430–435.
17 Tsuda M, *et al.* 2003. Conserved role of nanos proteins in germ cell development. *Science*. 301:1239–1241.
18 Fehilly CB, Willadsen SM, Tucker EM. 1984. Experimental chimaerism in sheep. *J Reprod Fertil*. 70:347–351.
19 Boediono A, *et al.* 1993. Production of chimeric calves by aggregation of in vitro-fertilized bovine embryos without zonae pellucidae. *Theriogenology*. 40:1221–1230.
20 Brem G, Tenhumberg H, Krausslich H. 1984. Chimerism in cattle through microsurgical aggregation of morulae. *Theriogenology*. 22:609–613.
21 Onishi A, Takeda K, Komatsu M, Akita T, Kojima T. 1994. Production of chimeric pigs and the analysis of chimerism using mitochondrial deoxyribonucleic acid as a cell marker. *Biol Reprod*. 51:1069–1075.
22 Gao X, *et al.* 2019. Establishment of porcine and human expanded potential stem cells. *Nat Cell Biol*. 21:687–699.
23 Zhao L, *et al.* 2021. Establishment of bovine expanded potential stem cells. *Proc Natl Acad Sci U S A*. 118:e2018505118.
24 Mahyari E, *et al.* 2024. The human infertility single-cell testis atlas (HISTA): an interactive molecular scRNA-seq reference of the human testis. *Andrology*. https://doi.org/10.1111/andr.13637.
25 Zhao L, *et al.* 2023. MHA, an interactive website for scRNA-seq data of male genitourinary development and disease. *Andrology*. 11:1157–1162.
26 Saba R, Kato Y, Saga Y. 2014. NANOS2 promotes male germ cell development independent of meiosis suppression. *Dev Biol*. 385:32–40.
27 Hochereau-de Reviers MT, Perreau C, Pisselet C, Locatelli A, Bosc M. 1995. Ontogenesis of somatic and germ cells in sheep fetal testis. *J Reprod Fertil*. 103:41–46.
28 You X, Chen Q, Yuan D, Zhang C, Zhao H. 2021. Common markers of testicular Sertoli cells. *Expert Rev Mol Diagn*. 21:613–626.
29 Chen H, Wang Y, Ge R, Zirkin BR. 2017. Leydig cell stem cells: identification, proliferation and differentiation. *Mol Cell Endocrinol*. 445:65–73.
30 Liebich A, *et al.* 2022. The molecular signature of human testicular peritubular cells revealed by single-cell analysis. *Cells*. 11:3685.
31 Liu X, *et al.* 2018. H3k9 demethylase KDM4E is an epigenetic regulator for bovine embryonic development and a defective factor for nuclear reprogramming. *Development*. 145:dev158261.
32 Matoba S, *et al.* 2014. Embryonic development following somatic cell nuclear transfer impeded by persisting histone methylation. *Cell*. 159:884–895.
33 Ohtsuka M, *et al.* 2012. Fluorescent transgenic mice suitable for multi-color aggregation chimera studies. *Cell Tissue Res*. 350:251–260.
34 Gardner RL, Cockroft DL. 1998. Complete dissipation of coherent clonal growth occurs before gastrulation in mouse epiblast. *Development*. 125:2397–2402.
35 Wood SA, Allen ND, Rossant J, Auerbach A, Nagy A. 1993. Non-injection methods for the production of embryonic stem cell-embryo chimaeras. *Nature*. 365:87–89.
36 Vandereyken K, Sifrim A, Thienpont B, Voet T. 2023. Methods and applications for single-cell and spatial multi-omics. *Nat Rev Genet*. 24:494–515.
37 Oback B, *et al.* Health and welfare of cloned ruminants. 2024. In: *IETS manual*. 4th ed. p. 151–169. https://www.iets.org/Publications/IETS-Manual.
38 McLean ZL, *et al.* 2021. Controlled cytoplast arrest and morula aggregation enhance development, cryoresilience, and in vivo survival of cloned sheep embryos. *Cell Reprogram*. 23:14–25.
39 Mulas C, *et al.* 2019. Defined conditions for propagation and manipulation of mouse embryonic stem cells. *Development*. 146:dev173146.
40 Vilarino M, *et al.* 2020. Derivation of sheep embryonic stem cells under optimized conditions. *Reproduction*. 160:761–772.
41 Bogliotti YS, *et al.* 2018. Efficient derivation of stable primed pluripotent embryonic stem cells from bovine blastocysts. *Proc Natl Acad Sci U S A*. 115:2090–2095.
42 Mclean Z, Oback B, Laible G. 2020. Embryo-mediated genome editing for accelerated genetic improvement of livestock. *Front Agr Sci Eng*. 7:148–160.
43 Wrenzycki C. In vitro production of (farm) animal embryos. 2018. In: Niemann H, Wrenzycki C, editors. *Animal biotechnology, vol. I reproductive biotechnologies*. Springer Life Sciences. p. 269–304.
44 Chen X, *et al.* 2010. Effect of microinjection of a single IVF-derived blastomere on the development of cloned embryos at the eight-cell stage in bovine. *Cell Reprogram*. 12:719–727.
45 Perisse IV, Fan Z, Singina GN, White KL, Polejaeva IA. 2020. Improvements in gene editing technology boost its applications in livestock. *Front Genet*. 11:614688.
46 Stemmer M, Thumberger T, Del Sol Keyer M, Wittbrodt J, Mateo JL. CCTop: an intuitive, flexible and reliable CRISPR/Cas9 target prediction tool. *PLoS One*. 10:e0124633.
47 Richardson CD, Ray GJ, DeWitt MA, Curie GL, Corn JE. 2016. Enhancing homology-directed genome editing by catalytically active and inactive CRISPR-Cas9 using asymmetric donor DNA. *Nat Biotechnol*. 34:339–344.
48 Brinkman EK, *et al.* 2018. Easy quantification of template-directed CRISPR/Cas9 editing. *Nucleic Acids Res*. 46:e58.
49 Li H. 26 March 2013. Aligning sequence reads, clone sequences and assembly contigs with BWA-MEM. arXiv 1303.3997. https://doi.org/10.48550/arXiv.1303.3997, preprint: not peer reviewed.
50 Li H, *et al.* 2009. The Sequence Alignment/Map format and SAMtools. *Bioinformatics*. 25:2078–2079.
51 Li H. 2011. A statistical framework for SNP calling, mutation discovery, association mapping and population genetical parameter estimation from sequencing data. *Bioinformatics*. 27:2987–2993.
52 McKenna A, *et al.* 2010. The Genome Analysis Toolkit: a MapReduce framework for analyzing next-generation DNA sequencing data. *Genome Res*. 20:1297–1303.
53 Rice P, Longden I, Bleasby A. 2000. EMBOSS: the European Molecular Biology Open Software Suite. *Trends Genet*. 16:276–277.
54 Concordet J-P, Haeussler M. 2018. CRISPOR: intuitive guide selection for CRISPR/Cas9 genome editing experiments and screens. *Nucleic Acids Res*. 46:W242–W245.

55 Thorvaldsdóttir H, Robinson JT, Mesirov JP. 2013. Integrative Genomics Viewer (IGV): high-performance genomics data visualization and exploration. *Brief Bioinform*. 14: 178–192.

56 Garrels W, *et al*. 2011. Germline transgenic pigs by Sleeping Beauty transposition in porcine zygotes and targeted integration in the pig genome. *PLoS One*. 6:e23573.

57 Mclean ZL, Appleby SJ, Fermin LM, Oback B. 2020. Generating cloned sheep embryos by zona-free somatic cell transfer. https://doi.org/10.17504/protocols.io.begbjbsn

58 Robertson I, Nelson RE. 1998. Certification and identification of the embryo. In: Stringfellow DA, Givens MD, editors. Manual of the International Embryo Technology Society: a procedural guide and general information for the use of embryo transfer technology. 5th ed. Champaign (IL): Publisher: International Embryo Technology Society. p. 86–105. 103–116.

59 Zoller DK, Vassiliadis PM, Voigt K, Sauter-Louis C, Zerbe H. 2015. Two treatment protocols for induction of preterm parturition in ewes—evaluation of the effects on lung maturation and lamb survival. *Small Rumin Res*. 124:112–119.